CrystEngComm

Cite this: *CrystEngComm*, 2012, **14**, 7345–7354

www.rsc.org/crystengcomm

PAPER

Self-assembly of alkyl *N*-acetylglyoxylic amides of varying chain lengths†

Venty Suryanti,‡*[ab] Mohan Bhadbhade,[b] Roger Bishop,[a] David StC Black[a] and Naresh Kumar*[a]

Received 21st June 2012, Accepted 27th July 2012
DOI: 10.1039/c2ce25994j

Alkyl *N*-acetylglyoxylic amides have been synthesised from *N*-acetylisatins and their self-assembly studied in the solid state by X-ray crystallography. Different molecular conformations were observed for molecules **5a**, **5b**, **5d** and **6b**, which have a strong influence on their supramolecular organization in the crystals. Both strong and weak interactions played key roles in the self-assembly process and the formation of well-defined supramolecular architectures. Crystal structures of **5b** revealed novel C=O···C=O (carbonyl–carbonyl) dipolar interactions involving three carbonyl groups and intermolecular halogen bonding interactions, either C–H···Br contacts with inclusion of cyclohexane in **5b-1** or Br···Br contacts without the inclusion of solvent in **5b-2**.

Introduction

Inter- and intramolecular interactions are recognised to be of fundamental importance to the self-assembly of supramolecules, crystal engineering and molecular recognition.[1] Particular emphasis has always been placed on strong hydrogen bond interactions (*e.g.* O–H···O and O–H···N), but there is now also increasing interest in the role played by weak interactions (*e.g.* π···π stacking, X–H···A (X = C, N, O; A = O, Cl, π) and halogen···halogen) and in elucidating how the cooperative action of these weak interactions influences molecular packing, crystal structure stability, molecular recognition and self-assembly processes.[2–4]

Carboxylic acids and amides are widely exploited in crystal engineering because they generate reliable dimeric and catemer supramolecular synthons *via* hydrogen bonding.[5–9] Conversely, the supramolecular synthons produced by glyoxylamides have received less attention. Greater versatility is offered by the use of glyoxylamides in self-assembly owing to the presence of the additional hydrogen bond accepting keto groups and the variable glyoxylamide torsional angle. For example, the self-assembly of indol-2-ylglyoxylamides was found to give dimeric structures exhibiting new hydrogen bonded motifs **1** and **2** (Fig. 1).[10] Unique intermolecular hydrogen bonding was also apparent in a related tertiary indol-7-ylglyoxylamide.[11]

Simple 2′-benzamidophenylglyoxylamides also self assemble by hydrogen bonding. The tertiary *N*-[2-(oxo-1-piperidinylacetyl)phenyl]acetamide exists as a monomer with strong hydrogen bonding between the single free amide NH proton and the α-carbonyl oxygen atom. This motif was also evident in the secondary *N*-[2-(2-oxobutanoyl)phenyl]benzamide, which exists as a dimer through additional hydrogen bonding between the benzamide carbonyl oxygen atom and the glyoxylamide NH proton.[12]

We are interested in the use of the glyoxylamide moiety in the development of peptidomimetics and have reported a facile ring opening reaction of *N*-acylisatins with amino acids and peptides to generate novel mono-, bis- and dendrimeric glyoxylamide derivatives that show antibacterial activity.[13–15] The non-proteinogenic amino acid 2-aminophenylglyoxylic acid unit allows for unique molecular conformations not shown by natural amino acids. During these studies we found the simple glycine peptidomimetic derivative **3** self-assembled into a dimer in a similar manner to the reported 2′-benzamidophenylglyoxylamides (Fig. 2). Strong intermolecular hydrogen bonding was

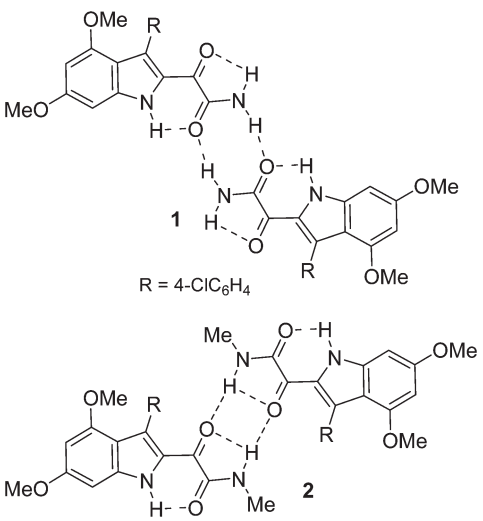

Fig. 1 Supramolecular synthons of indol-2-ylglyoxylamides.

[a]*School of Chemistry, The University of New South Wales, Sydney, NSW, 2052, Australia. E-mail: n.kumar@unsw.edu.au*
[b]*Mark Wainwright Analytical Centre, The University of New South Wales, Sydney, NSW, 2052, Australia*
† Electronic supplementary information (ESI) available. CCDC reference numbers 887275–887279. For ESI and crystallographic data in CIF or other electronic format see DOI: 10.1039/c2ce25994j
‡ On leave from Department of Chemistry, The University of Sebelas Maret, Surakarta, Jawa Tengah, 57126, Indonesia. *E-mail:* venty@mipa.uns.ac.id

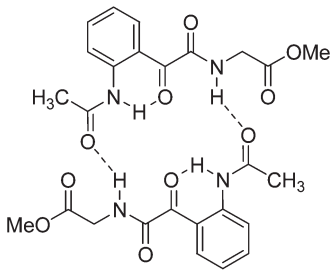

3

Fig. 2 Hydrogen bonding motifs between molecules of peptidomimetic **3**.

evident between the gloxylamide NH proton and the acetamide oxygen atom. Intramolecular hydrogen bonding was also evident between the acetamide NH proton and the α-carbonyl oxygen atom.

As an extension of this work we now report our initial findings into the self-assembly behaviour of these 2-aminophenylglyoxylic acid moieties. Alkyl side chains have been reported to promote hydrophobic aggregation through van der Waals forces,[16–17] so our particular interest was in the development of more amphiphilic analogues of **3**, bearing longer alkyl and ester alkyl chains, which could potentially display enhanced gelation and self-assembly properties.

Results and discussion

The first synthetic targets prepared were the simple alkyl substituted 2′-acetylamidophenylglyoxylamides **5**. Accordingly, *N*-acetylisatins **4** were heated at reflux for 4 h in dichloromethane with hexylamine, dodecylamine or octadecylamine to give analogues **5a–i** in 42–84% yield after column chromatography (Scheme 1, Table 1).

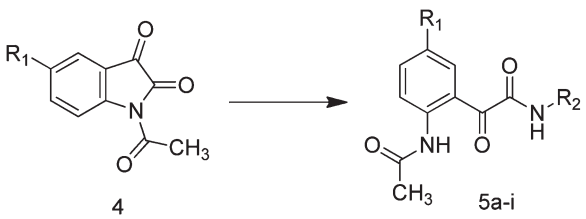

4 **5a-i**

Scheme 1 *Reagents and conditions*: amine, CH_2Cl_2, reflux, 4 h.

Table 1 Synthesis of 2′-acetylamidophenylglyoxylamides **5**

Entry	Product	R_1	R_2	Yield[a] (%)
1	**5a**	H	$(CH_2)_5CH_3$	48
2	**5b**	Br	$(CH_2)_5CH_3$	55
3	**5c**	CH_3	$(CH_2)_5CH_3$	68
4	**5d**	H	$(CH_2)_{11}CH_3$	72
5	**5e**	Br	$(CH_2)_{11}CH_3$	84
6	**5f**	CH_3	$(CH_2)_{11}CH_3$	76
7	**5g**	H	$(CH_2)_{17}CH_3$	42
8	**5h**	Br	$(CH_2)_{17}CH_3$	70
9	**5i**	CH_3	$(CH_2)_{17}CH_3$	60

[a] Isolated yield (reaction was not optimized).

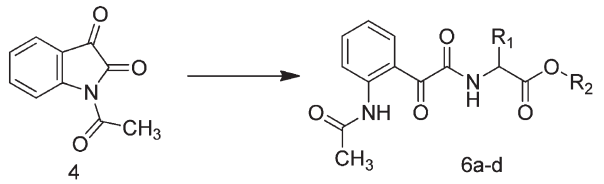

4 **6a-d**

Scheme 2 *Reagents and conditions*: amino acid alkyl ester hydrochloride salt, $NaHCO_3$, CH_2Cl_2/H_2O (1 : 1 v/v), 0 °C to r.t., 24 h.

The second synthetic targets of interest were the related alkyl substituted 2′-acetylamidophenylglyoxylamide peptide derivatives **6**. The introduction of a hydrophilic amino acid to the side chain of these structures was anticipated to enhance the hydrogen bonding interactions and hence aggregation of these compounds. In accordance with our reported methodology,[9] *N*-acetylisatin **4** was stirred in dichloromethane for 24 h with an amino acid alkyl ester and sodium hydrogen carbonate, initially at 5 °C and then gradually warmed to room temperature. Glycine butyl ester hydrochloride, glycine hexyl ester hydrochloride, L-alanine butyl ester hydrochloride and L-alanine hexyl ester hydrochloride were selected as representative amino acid alkyl esters. The resulting peptidomimetics **6a–d** were isolated in 45–67% yield upon workup (Scheme 2, Table 2).

Glyoxylamides **5a–i** and **6a–d** were subsequently recrystallized from a range of solvents including hexane, cyclohexane, methanol, ethanol, dichloromethane/hexane and acetonitrile *via* slow evaporation of the solvent at room temperature. Crystals suitable for X-ray structure determination were successfully obtained for compounds **5a**, **5b**, **5d** and **6b**. The other compounds afforded only amorphous solids.

Crystal structures of 5a, 5b, 5d and 6b

Single crystal X-ray structure determinations were carried out on compounds **5a**, **5b 5d** and **6b** and a summary of crystallographic data is provided in Table 3. The *R* factors for structures **5a** and **5d** from synchrotron data are somewhat higher as compared to the rest of the structures, but structural parameters are all normal and therefore allow us to include them for our discussion here. Conformationally flexible side chains exhibited disorder in structures **5b-1**, **5b-2** and **5d** (details in the ESI†). These crystal structures are grouped in two categories based on their intramolecular strong and weak interactions. The crystal structures are shown in Fig. 3 depicting these intramolecular interactions. The molecular conformations are different in these two groups of molecules and have a strong influence on their supramolecular organization.

The first group, **5a**, **5d** and **6b**, contains an intramolecular N–H···O hydrogen bond that is formed by O2A as an acceptor

Table 2 Synthesis of 2′-acetylamidophenylglyoxylamide peptidomimetics **6**

Entry	Amino acid[a]	Product	R_1	R_2	Yield[b](%)
1	Glycine	**6a**	H	$(CH_2)_3CH_3$	52
2	Glycine	**6b**	H	$(CH_2)_5CH_3$	45
3	L-Alanine	**6c**	CH_3	$(CH_2)_3CH_3$	63
4	L-Alanine	**6d**	CH_3	$(CH_2)_5CH_3$	67

[a] As the alkyl ester hydrochloric salt. [b] Isolated yield (reaction was not optimized).

Table 3 Crystal data collection and structure refinement parameters of **5a**, **5d**, **6b**, **5b-1**, and **5b-2**

Compound	**5a**	**5d**	**6b**	**5b-1**	**5b-2**
Chemical formula	$C_{16}H_{22}N_2O_3$	$C_{22}H_{34}N_2O_3$	$C_{18}H_{24}N_2O_5$	$C_{16}H_{21}BrN_2O_3{\cdot}(C_6H_{12})_{0.5}$	$C_{16}H_{21}BrN_2O_3$
M_r	290.36	374.51	348.39	411.34	369.26
Crystal system	Monoclinic	Monoclinic	Monoclinic	Triclinic	Triclinic
Space group	$P2_1/c$	$P2_1/c$	$P2_1$	$P\bar{1}$	$P\bar{1}$
T/K	100	100	155	150	150
a, b, c/Å	36.447 (7), 5.012 (1), 17.294 (4)	24.240 (5), 5.021 (1), 17.387 (3)	5.0331 (3), 33.007 (2), 5.5043 (3)	8.8992 (12), 9.9071 (17), 12.299 (2)	8.5713 (11), 9.9041 (11), 11.2296 (14)
α, β, γ (°)	90, 103.65 (3), 90	90, 91.28 (3), 90	90, 99.240 (4), 90	75.265 (7), 81.633 (7), 76.227 (7)	97.717 (4), 108.250 (4), 101.874 (4)
V/Å^3	3069.8 (11)	2115.6 (7)	902.55 (9)	1014.4 (3)	865.48 (18)
Z	8	4	2	2	2
μ/mm^{-1}	0.09	0.10	0.09	2.05	2.39
Crystal size/mm	0.10 × 0.04 × 0.03	0.10 × 0.02 × 0.02	0.34 × 0.23 × 0.04	0.37 × 0.08 × 0.08	0.14 × 0.06 × 0.04
T_{min}, T_{max}	Absorption corrections are not applied	Absorption corrections are not applied	0.969, 0.996	0.522, 0.849	0.726, 0.902
No. of measured, independent and observed [$I > 2\sigma(I)$] reflections	31 592, 5360, 4467	24 994, 3480, 3413	6437, 3076, 2899	12 828, 3548, 2328	11 690, 3012, 2430
R_{int}	0.102	0.034	0.022	0.079	0.049
$R[F^2 > 2\sigma(F^2)]$, w$R(F^2)$, S	0.200, 0.452, 1.16	0.130, 0.410, 1.05	0.030, 0.069, 1.35	0.061, 0.189, 1.10	0.040, 0.129, 0.89
No. of reflections	5360	3480	3076	3548	3012
No. of parameters	383	300	228	264	228
No. of restraints	0	356	1	83	30
$\Delta\rangle_{max}$, $\Delta\rangle_{min}$/e Å^{-3}	1.00, −0.74	0.74,−0.83	0.13, −0.16	0.51, −0.65	0.62, −0.56

and N1A–H1A and N2A–H2A as the two donor groups. Similarly the oxygen O3A accepts protons from two C–H groups, namely C3–H3 and C11-–H11. In molecule **5d**, the oxygen O3A accepts protons from three C–H groups, namely C3–H3, C11–H11 and C12–H12B. In addition, there is an extra C–H···O bond, C6–H6···O1 (Fig. 3 (a–c) and Tables 4–6).

In the second group, two crystal forms of **5b** were produced: **5b-1** containing cyclohexane, and solvent free **5b-2** that was crystallised from hexane. Both structures showed an absence of the intramolecular N1–H1···O2 hydrogen bond interactions which was characteristic in the previous group. In both crystal forms of **5b**, the moieties C7=O1, N1–H1 and C9=O2, C10=O3 and N2–H2 are almost reversed by rotating ∼180° with respect to the conformations in group 1. The overlap of the five structures (Fig. 3f) shows the conformational differences among them. This striking conformational difference in the structures brings three carbonyl groups to form a cluster that shows dipolar contacts among them. Thus, carbonyl group C7=O1 makes short contacts with the carbons C9 and C10 of the two carbonyl groups C9=O2 and C10=O3 respectively. As a result, the intra C6–H6···O1 bond in group 1 is absent here. Atom O2 acts as an acceptor to groups C3–H3 and N2–H2N. In addition, O3 forms a single C–H···O type contact with C11–H11 of the side chain in both **5b-1** and **5b-2** and with a possible weaker contact from C12–H12 in **5b-2** (Fig. 3 (d) and (e)). Numerical details of the molecular interactions present in the crystal forms are listed in Tables 7–8.

Both the antiparallel and orthogonal carbonyl–carbonyl dipolar interactions are known to be able to compete effectively with strong hydrogen bonds in crystal packing.[18] The antiparallel interaction is more subject to molecular steric effects and therefore the orthogonal motif is encountered more frequently,[19] especially in crystal structures of proteins and other amide-containing compounds.[20,21] 1,2-Dicarbonyl groups usually adopt a transoid conformation,[22] as is the case for the five glyoxylamide crystal structures described here. However, the intramolecular triple orthogonal carbonyl dipolar interaction present in the structures **5b-1** and **5b-2** is novel and has not previously received any attention.

Supramolecular organization

The glyoxylamides (**5a**, **5b**, **5d** and **6b**) comprise an aromatic head group and associated side chains. The group 1 structures have some features in common (Fig. 4a–c), whereas the bromo derivative **5b**, because of halogen interactions predominating in the molecular organization, differs sharply from these (Fig. 4d–e). The shorter alkyl chain in **5a** (with 6 carbon atoms) shows a slightly bent conformation whereas the longer chain compounds **6b** (glycine ester added to the 6 carbon chain) and **5d** (12 carbon atoms) have essentially extended chain conformations with interchain separation of approximately 4 Å. The longer chain lengths in **5d** and **6b** resulted in highly packed structures due to extensive van der Waals interactions between the alkyl chains. Conversely, the shorter chain lengths in **5a** showed less dense supramolecular structures.

Amongst the first group, the compound **6b** shows a difference in the supramolecular organization from the other two structures; the head···head association seen in **5a** and **5d** is absent in **6b**. The reasons for this are best understood from the close up view of the interactions in these structures (Fig. 5). The responsible factor is the addition of glycine in the alkyl chain that restricts the free rotation of the side chain, possibly due to the presence of C=O···C=O (carbonyl–carbonyl) dipolar interactions. Interdigitating alkyl chains were observed in **5a** and **5d**, whereas parallel alkyl chains were seen in **6b**.

The crystal structure of **5a** contains two crystallographically independent molecules (A and B, shown in blue and green, respectively). The association between these molecules occurs

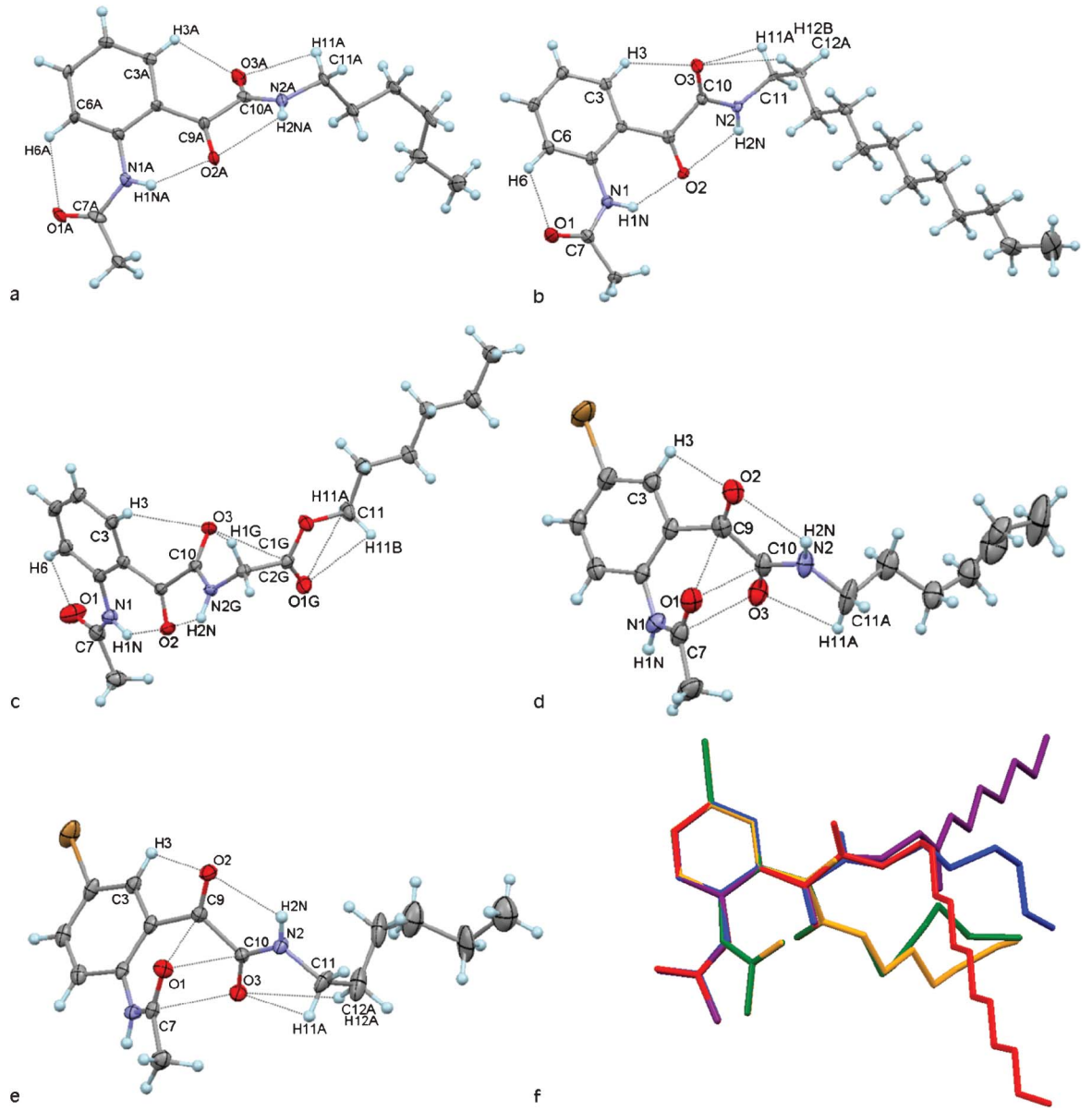

Fig. 3 Intramolecular interactions present in molecule: (a) **5a**, (b) **5d**, (c) **6b**, (d) **5b-1**, (e) **5b-2**, and (f) structure overlay of all five structures showing conformational differences (colour codes: **5a**: blue; **5d**: red; **6b**: purple; **5b-1**: dark green and **5b-2**: yellow). Disordered atoms of the side chains are omitted for clarity reasons.

Table 4 Numerical details of the intramolecular interactions present in **5a**

Donor (D)–H···Acceptor (A)	D–H (Å)	H···A (Å)	D···A (Å)	Angle (°)
N1A–H1NA···O2A=[C9A]	0.86	2.02	2.653(11)	130
N2A–H2NA···O2A=[C9A]	0.86	2.36	2.691(11)	103
C3A–H3A···O3A=[C10A]	0.93	2.44	2.938(13)	113
C11A–H11A···O3A=[C10A]	0.97	2.48	3.236(17)	98
C6A–H6A···O1A=[C7A]	0.93	2.32	2.891(12)	119
N1B–H1NB···O2B=[C9B]	0.86	2.04	2.656(13)	128
N2B–H2NB···O2B=[C9B]	0.86	2.41	2.699(11)	100
C3B–H3B···O3B=[C10B]	0.93	2.45	2.909(14)	111
C11B–H11C··· O3B=[C10B]	0.97	2.55	3.251(16)	95
C6B–H6B···O1B=[C7B]	0.93	2.30	2.863(12)	119

through CH···O contacts, namely C16B–H16F···O2A and C16A–H16B···O2B. Molecules A (or molecules B) are connected to each other by strong intermolecular hydrogen bonds, N2–H2N···O3=C10 with *d*(N···O) of 2.764 Å and the angle N–H···O

Table 5 Numerical details of the intramolecular interactions present in **5d**

Donor (D)–H···Acceptor (A)	D–H (Å)	H···A (Å)	D···A (Å)	Angle (°)
N1–H1N···O2=[C9]	0.86	1.96	2.660(6)	138
N2–H2N···O2=[C9]	0.86	2.38	2.684(6)	101
C3–H···O3=[C10]	0.93	2.45	2.932(6)	112
C11H11A···O3=[C10]	0.97	2.69	2.781(6)	85
C12AH12B···O3=[C10]	0.97	2.62	3.139(6)	114
C6–H···O1=[C7]	0.93	2.29	2.888(6)	122

Table 6 Numerical details of the intramolecular interactions present in **6b**

Donor (D)–H···Acceptor (A)	D–H (Å)	H···A (Å)	D···A (Å)	Angle (°)
N1–H···O2= [C9]	0.88	1.98	2.683(2)	137
N2G–H2N···O2= [C9]	0.88	2.53	2.770(2)	97
C3–H···O3= [C10]	0.95	2.48	2.954(2)	111
C1GH1G···O3= [C10]	0.99	2.65	2.700(2)	82
C6–H6···O1= [C7]	0.95	2.27	2.873(2)	121
C1H11A···O1G=C2G	0.99	2.56	2.639(2)	83
C1H11B···O1G=C2G	0.99	2.64	2.639(2)	79

C=O···C=O	O···C (Å)	C=O···C (°)	O···C=O (°)
C10=O3···C2G=O1G	2.895(2)	81.67(12)	101.45(12)

of *ca*. 145°. In addition, weak intermolecular hydrogen bonding was also observed; O1 accepts protons from two C–H groups, namely C5–H5 and C8–H8 with *d*(C···O) of 3.267 and 3.494 Å, respectively (Fig. 5a and Table 9).

In the crystal structure of **5d**, O3 acts as an acceptor for two protons, which are N2–H2 forming strong intermolecular hydrogen bonds with *d*(N···O) of 2.788(6) Å and C11–H11B forming a weak intermolecular hydrogen bonds with *d*(C···O) of 3.226(6) Å. The same weak intermolecular hydrogen bonding present in **5a** was also observed in **5d**, where oxygen O1 accepts protons from two C–H groups, namely C5–H5 and C8–H8, with *d*(C···O) of 3.278(6) and 3.315(6) Å, respectively (Fig. 5b and Table 10).

In the crystal structure of **6b**, O3 acts as an acceptor for two protons, with N2G–H2N forming strong intermolecular hydrogen bonds with *d*(N···O) of 2.801(1) Å and CG–H21B forming weak intermolecular hydrogen bonds with *d*(C···O) of 3.192(2) Å. A different type of weak head to tail intermolecular hydrogen bonding was observed in **6b**, where oxygen O1 accepts protons from two C–H groups, namely C8–H8 and C16–H16A, from the end of the alkyl side chain of the molecules in the adjacent row with *d*(C···O) of 3.352 (2) and 3.365(7) Å, respectively (Fig. 5c and Table 11).

The bromo derivative **5b** produced two crystal forms, one without the solvent (**5b-2**) and one with the solvent (**5b-1**). The identical H-bonded one dimensional molecular rows are packed differently in the two unit cells; closer packing of these rows in structure **5b-2** does not leave any voids, whereas in **5b-1**, larger separation of these rows creates channels that are occupied by the solvent molecule cyclohexane (Fig. 6a). There is one-dimensional isostructurality[23–26] between the two structures,

Table 7 Numerical details of the intramolecular interactions present in **5b-1**

Donor (D)–H···Acceptor (A)	D–H (Å)	H···A (Å)	D···A (Å)	Angle (°)
N2–H···O2= [C9]	0.88	2.33	2.690(6)	104
C3–H···O2= [C9]	0.95	2.54	2.814(6)	97
C11A–H11A···O3= [C10]	0.99	2.50	2.805(6)	97

C=O···C=O	O···C (Å)	C=O···C (°)	O···C=O (°)
C7=O1···C9=O2	2.558(6)	103.7(1)	105.71(1)
C7=O1···C10=O3	2.841(6)	88.0(1)	106.5(1)
C10=O3···C7=O1	3.148(6)	74.3(1)	91.1(1)

Table 8 Numerical details of the intramolecular interactions present in **5b-2**

Donor (D)–H···Acceptor (A)	D–H (Å)	H···A (Å)	D···A (Å)	Angle (°)
N2–H···O2= [C9]	0.88	2.34	2.700(4)	104
C3–H···O2= [C9]	0.95	2.55	2.829(4)	97
C11A–H11A···O3= [C10]	0.99	2.67	2.805(4)	86
C12A–H12A···O3= [C10]	0.99	2.64	3.169(4)	114

C=O···C=O	O···C (Å)	C=O···C (°)	O···C=O (°)
C7=O1···C9=O2	2.548(4)	104.7(1)	105.9(1)
C7=O1···C10=O3	2.832(4)	89.2(1)	104.9(1)
C10=O3···C7=O1	3.133(4)	75.7(1)	90.1(1)

despite their differences in the flexible side chain conformations. The intermolecular N–H···O hydrogen bonding across a centre of inversion doubly bridges two neighbouring molecules along the *b*-axis of the monoclinic space group in both structures (Fig. 6b, Tables 12 and 13). Although there is one dimensional isostructurality in these two crystal forms, these 1D chains are associated differently in the other dimensions due to different interactions made by the halogen, Br (Fig. 6c). Crystal structure **5b-2** shows linear chain Br···Br short contacts with Br···Br contact distance of 3.531(1) Å and slipped π···π contacts between the aromatic groups (Fig. 5). In contrast, structure **5b-1** forms a pseudo-macrocycle using two identical C–H···Br interactions with *d*(H···Br) of 3.09 Å, *d*(C···Br) of 4.063 Å and angle C–H···Br *ca*. of 173°. The cyclohexane guest is trapped at the centre of this macrocycle using two identical bifurcated C–H···π contacts with the aromatic ring and the carbonyl group (Fig. 6c). It is noteworthy that the cyclohexane guest makes weaker C–H···π contacts with the host, rather than using options of C–H···Br or even C–H···O hydrogen bonding to form a stable inclusion crystal.

Conclusions

A number of alkyl *N*-acetylglyoxylamides were successfully prepared by ring-opening of *N*-acetylisatins with a range of amines. X-ray crystallography studies of the synthesised molecules revealed different types of crystal packing for compounds **5a**, **5b**, **5d** and **6b**. A cooperative effect between strong and weak interactions played an important role in directing the packing of these molecules during crystallization.

Structures **5a**, **5d**, **6b** and the parent glycine peptidomimetic derivative **3** displayed characteristic N1–H1···O2 hydrogen bond interactions which may represent a potential supramolecular synthon in the crystallization of 2-aminophenylglyoxylic acid based peptidomimetics. Conversely, novel intramolecular triple orthogonal carbonyl dipolar interactions were observed in structures **5b-1** and **5b-2**. In many molecules, halogen atoms often make short contacts with a variety of other atoms, including halogen–halogen ($X_1 \cdots X_2$) interactions, which play a significant role in determining the crystal structures.[27-30] This is certainly the case for molecule **5b**, where the halogen atom either uses a C–H···Br type interaction (**5b-1**) or a Br···Br type interaction (**5b-2**). Introduction of the alkyl side chains was found to enhance the self-assembly properties of these aminophenylglyoxylic acids, which no longer favoured the dimeric conformation displayed by the parent compound **3**.

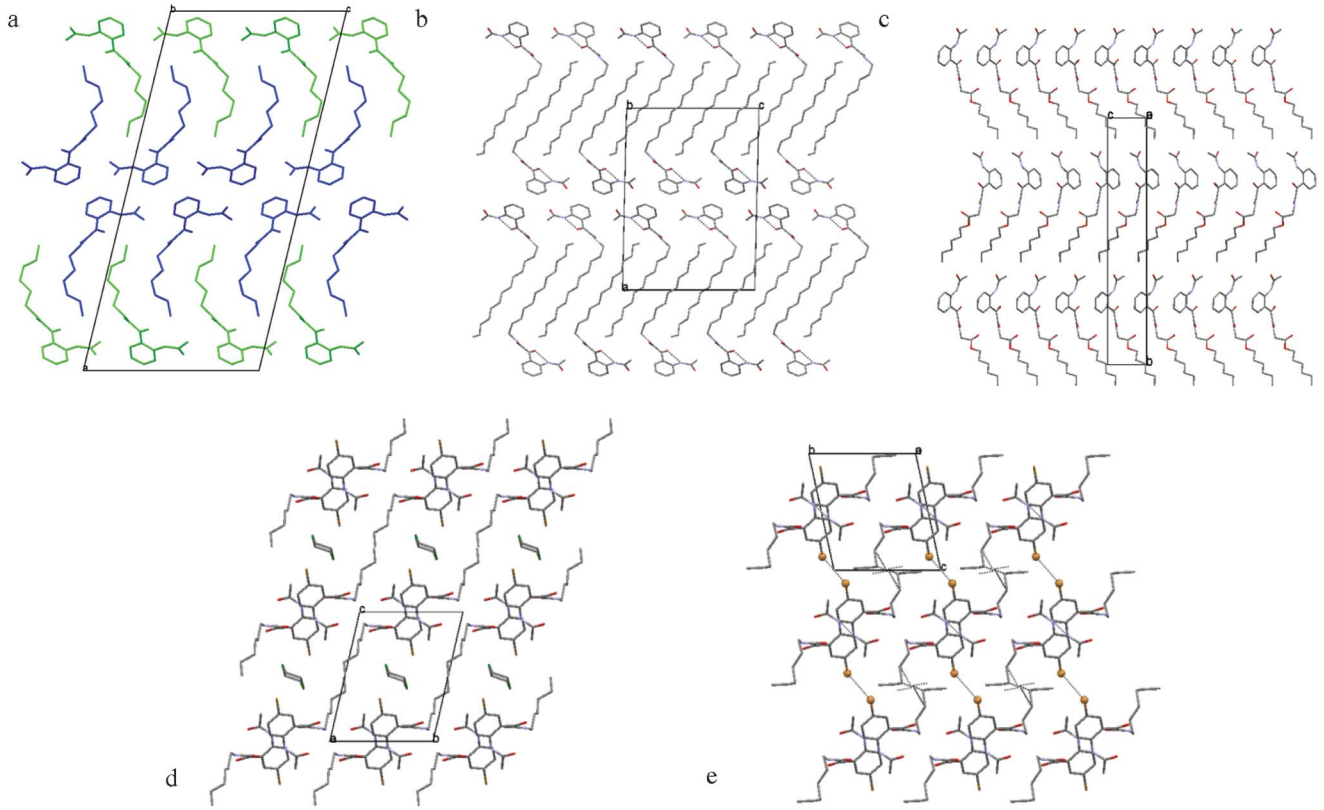

Fig. 4 Crystal packing of (a) **5a**, (b) **5d**, (c) **6a**, (d) **5b-1**, and (e) **5b-2**.

The self-assembly of substituted glyoxylamides is a complex area which remains relatively unexplored. Further studies in this area are ongoing in order to fully eludicate the factors which control this process in the solid state.

Experimental

Physical measurements

NMR data were recorded using a Bruker DPX300 instrument (^{1}H 300 MHz, ^{13}C 75.4 MHz) at 25 °C and reported as chemical shift (δ) relative to $SiMe_4$. Carbon substitution information was determined using the DEPT procedure, and the IR spectra were recorded using a Perkin–Elmer PE298 spectrophotometer with the sample prepared as a KBr pellet, in the range 4000–400 cm^{-1}.

Structure determination

Suitable single crystals of **5b** and **6b**, selected under the polarizing microscope (Leica M165Z), were picked up on a MicroMount (MiTeGen, USA) consisting of a thin polymer tip with a wicking aperture. The X-ray diffraction measurements were carried out on a Bruker KAPPA APEX II CCD diffractometer at 150 K by using graphite-monochromated Mo-Kα radiation (λ = 0.710723 Å). The single crystals, mounted on the goniometer using cryo loops for intensity measurements, were coated with paraffin oil and then quickly transferred to the cold stream using an Oxford Cryo stream attachment. Symmetry related absorption corrections using the program SADABS[31] were applied and the data were corrected for Lorentz and polarisation effects using Bruker APEX2 software.[32] All structures were solved by direct methods and the full-matrix least-squares refinements were carried out using SHELXL.[33] The non-hydrogen atoms were refined anisotropically. The molecular graphics were generated using Mercury.[34]

The X-ray diffraction measurements for **5a** and **5d** were carried out at MX1 and MX2 beamlines at the Australian Synchrotron Facility, Melbourne. The procedure for diffraction intensity measurements on both beam lines was similar. The crystal was mounted on the goniometer using a cryo loop for diffraction measurements, coated with paraffin oil and then quickly transferred to the cold stream using Cryo stream attachment. Data were collected using Si<111> monochromated synchrotron X-ray radiation (λ = 0.71023 Å) at 100(2) K and were corrected for Lorentz and polarization effects using the XDS software.[35] The structure was solved by direct methods and the full-matrix least-squares refinements were carried out using SHELXL.[33]

Synthesis

GP 1: General procedure for the synthesis of *N*-acetyl glyoxylicamides 5a–i. Alkylamine (1.0 mmol) was added to a stirred solution of *N*-acetylisatin (1.0 mmol) in CH_2Cl_2 (10 mL) and the mixture was heated at reflux for 4 h. After cooling to room temperature, the solvent was evaporated under reduced pressure and the crude product was purified by column chromatography using silica gel and a mixture of hexane and

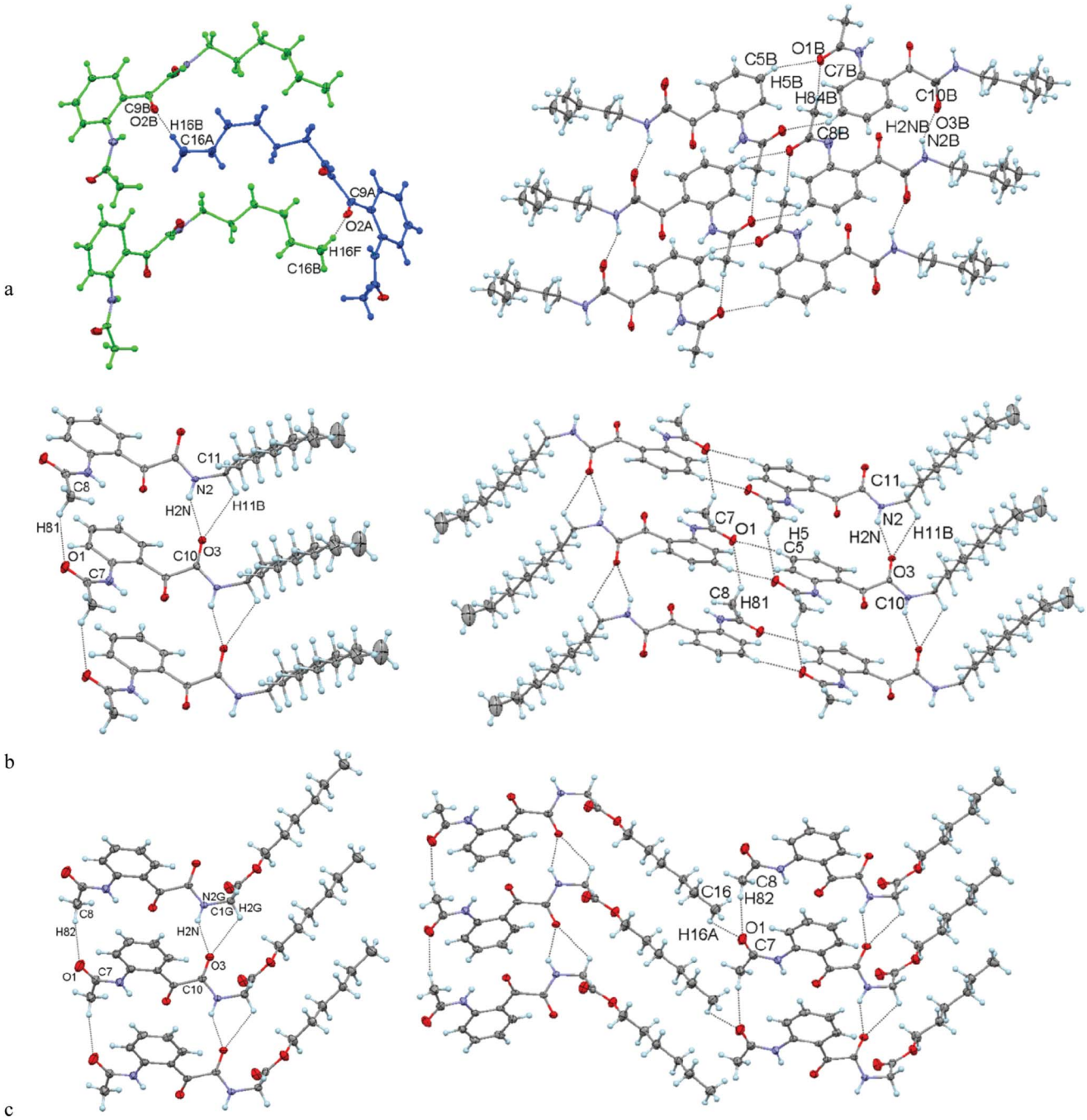

Fig. 5 Intermolecular interactions present in (a) **5a**, (b) **5d**, and (c) **6b**.

dichloromethane as eluent. The product was recrystallized from n-hexane and dried in vacuo.

GP 2: General procedure for the synthesis of *N*-acetyl glyoxylamide peptide mimics 6a–d. A solution of amino acid ester hydrochloride (2.5 mmol) containing saturated $NaHCO_3$ was added to a stirred solution of the *N*-acetylisatin (1.0 mmol) in CH_2Cl_2 (10 mL) at 5 °C. The reaction mixture was warmed to room temperature and stirred for 24–28 h. The organic layer was diluted with CH_2Cl_2 (20 mL) and extracted with aqueous HCl (0.5 M, 15 mL) and water (20 mL). The organic extract was dried over anhydrous Na_2SO_4, filtered and concentrated under vacuum.

2-(2-Acetamidophenyl)-*N*-hexyl-2-oxoacetamide, 5a. *N*-Acetylglyoxylic amide **3a** was prepared from 1-acetylindoline-2,3-dione (0.38 g, 2 mmol) and hexylamine (0.21 g, 2 mmol) according to GP 1. The title compound **5a** was afforded as white flakes after purification by column chromatography (0.28 g, 48%). The solid, recrystallized from CH_3CN *via* slow evaporation of the solvent at room temperature, yielded crystals suitable for X-ray crystal structure determination. **5a**: mp 114–116 °C; UV (MeOH): λ_{max} 200 nm (ε 18 845 cm^{-1} M^{-1}), 233 (21 882), 267 (7495), 339 (2826); IR (KBr): ν_{max} 3265, 3120, 3054, 2951, 2931, 2853, 1665, 1606, 1536, 1484, 1466, 1432, 1367, 1321, 1300, 1279, 1259, 1234, 1210, 1160, 1114, 1013, 969, 896, 814, 764, 707,

Table 9 Numerical details of the intermolecular interactions present in **5a**

Donor (D)–H···Acceptor (A)	D–H (Å)	H···A (Å)	D···A (Å)	Angle (°)
N2A–H2NA···O3A[a]=[C10A]	0.86	2.06	2.805(13)	144
C5A–H5A···O1A[c] =[C7A]	0.93	2.43	3.267(13)	113
C8A–H8A···O1A[a]=[C7A]	0.96	2.36	3.221(17)	148
C16A–H16B[e]···O2B[f]=[C9B]	0.96	2.65	3.494(16)	150
N2B–H2NB···O3B[b]=[C10B]	0.86	2.01	2.764(14)	145
C5B–H5B···O1B[d] =[C7B]	0.93	2.43	3.270(15)	150
C8B–H8B···O1B[b]=[C7B]	0.96	2.30	3.246(13)	170
C16B–H16F[g]···O2A[h]=[C9A]	0.96	2.65	3.519(15)	150

Equivalent position indicators:[a] $x, -1 + y, z$. [b] $x, 1 + y, z$. [c] $-x, 2 - y, -z$. [d] $1 - x, -y, -z$. [e] $x, 1 + y, z$. [f] $x, 2.5 - y, ½ + z$. [g] x, y, z. [h] $x, 1 + y, z$.

669, 648, 603, 561, 518 cm^{-1}; ^1H NMR (300 MHz, $CDCl_3$): δ 0.90 (t, J = 6.84 Hz, 3H, $CH_2(CH_2)_4CH_3$), 1.29–1.44 (m, 6H, $CH_2CH_2(CH_2)_3CH_3$), 1.56–1.66 (m, 2H, $NHCH_2CH_2(CH_2)_3CH_3$), 2.24 (s, 3H, $COCH_3$), 3.38–3.45 (m, 2H, $NHCH_2CH_2(CH_2)_3CH_3$), 6.91 (s, 1H, CONH), 7.11–7.17 (m, 1H, H4), 7.59–7.65 (m, 1H, H5), 8.41 (dd, J = 1.51, 8,11 Hz, 1H, H3), 8.67 (dd, J = 8.60, 0.88, Hz, 1H, H6), 10.96 (s, 1H, NHCO); ^{13}C NMR (75.6 MHz, $CDCl_3$): δ 192.21, 169.19, 162.84 (3 × C=O), 141.93 (ArC), 136.38 (ArCH), 134.30 (ArCH), 122.47 (ArCH), 120.57 (ArCH), 118.65 (ArC), 39.55 ($NHCH_2$), 31.29, 29.14, 26.44, 22.43 ($CH_2(CH_2)_4CH_3$), 25.43 ($COCH_3$), 13.90 ($CH_2(CH_2)_4CH_3$); HRMS (ESI) *m/z* calculated for $C_{16}H_{22}N_2O_3$ $(M + 1)^+$ 291.1630. Found 291.1696; Anal. Calcd. for $C_{16}H_{22}N_2O_3$: C, 66.18; H, 7.64; N, 9.65. Found: C, 66.29; H, 7.76; N, 9.59%.

2-(2-Acetamido-5-bromophenyl)-*N*-hexyl-2-oxoacetamide, 5b. The *N*-acetylglyoxylic amide **5b** was prepared from 1-acetyl-5-bromoindoline-2,3-dione (0.40 g, 1.5 mmol) and hexylamine (0.15 g, 1.5 mmol). according to GP 1. The title compound **5b** was afforded as a light brown solid after purification by column chromatography (0.61 g, 55%). The solid, recrystallized from hexane or cyclohexane *via* slow evaporation of the solvent at room temperature, yielded crystals suitable for X-ray crystal structure determination. **5b**: mp 116–118 °C; UV (MeOH): λ_{max} 203 nm (ε 31 023 cm^{-1} M^{-1}), 238 (32 886), 345 (3000); IR (KBr): ν_{max} 3277, 2955, 2927, 2850, 1664, 1599, 1521, 1482, 1369, 1293, 1258, 1203, 1137, 822, 693 cm^{-1}; ^1H NMR (300 MHz, $CDCl_3$): δ 0.91 (t, J = 6.76 Hz, 3H, $CH_2CH_2(CH_2)_3CH_3$), 1.25–1.44 (m, 6H, $CH_2CH_2(CH_2)_3CH_3$), 1.56–1.66 (m, 2H, $CH_2CH_2(CH_2)_3CH_3$), 2.21 (s, 3H, $COCH_3$), 3.36–3.43 (m, 2H, $NHCH_2(CH_2)_4CH_3$), 6.95 (s, 1H, CONH), 7.66 (dd, J = 2.41, 9.08 Hz, 2H, H6), 8.53 (d, J = 7.04 Hz, 1H, H5), 8.56 (s, 1H, H3), 10.84 (s, 1H, NHCO); ^{13}C NMR (75.6 MHz, $CDCl_3$): δ 190.66, 169.10, 161.91 (3 × C=O), 140.76 (ArC), 138.91 (ArCH), 136.40 (ArCH), 122.30 (ArCH), 120.29 (ArCH), 114.94 (ArC), 39.66 ($NHCH_2$), 31.29, 29.09, 26.44, 22.43 ($CH_2(CH_2)_4CH_3$), 25.33 ($COCH_3$), 13.91 ($CH_2(CH_2)_4CH_3$); HRMS (ESI) *m/z* calculated for $C_{16}H_{21}BrN_2O_3$ $(M + 1)^+$ 369.0736. Found 369.0791; Anal. Calcd. for $C_{16}H_{21}BrN_2O_3$: C, 52.04; H, 5.73; N, 7.59. Found: C, 52.26; H, 5.94; N, 7.53%.

Table 10 Numerical details of the intermolecular interactions present in **5d**

Donor (D)–H···Acceptor (A)	D–H (Å)	H···A (Å)	D···A (Å)	Angle (°)
N2–H···O3[a]=[C10]	0.86	2.04	2.788(6)	144
C11–H11···O3[a]=[C10]	0.97	2.70	3.226(6)	115
C5–H···O1[b]=[C7]	0.93	2.46	3.278(6)	147
C8–H···O1[b]=[C7]	0.96	2.50	3.315(6)	133

Equivalent position indicators:[a] $x, -1 + y, z$. [b] $1 - x, 2 - y, 1 - z$.

Table 11 Numerical details of the intermolecular interactions present in **6b**

Donor (D)–H···Acceptor (A)	D–H (Å)	H···A (Å)	D···A (Å)	Angle (°)
N2G–H···O3[a]=[C10]	0.88	2.07	2.801(1)	139
C1G–H2G···O3[a]=[C10]	0.99	2.65	3.192(2)	115
C8–H82···O1[a]=[C7]	0.98	2.39	3.352(3)	166
C16–H16A···O1[a]=[C7]	0.98	2.77	3.365(3)	120

Equivalent position indicators:[a] $-1 + x, y, z$.

2-(2-Acetamidophenyl)-*N*-dodecyl-2-oxoacetamide, 5d. *N*-Acetylglyoxylic amide **5d** was prepared from 1-acetylindoline-2,3-dione (0.28 g, 1.5 mmol) and dodecylamine (0.28 g, 1.5 mmol) according to GP 1. The title compound **5d** was afforded as off-white flakes (0.41 g, 72%). The solid, recrystallized from hexane *via* slow evaporation of the solvent at room temperature, yielded crystals suitable for X-ray crystal structure determination. **5d**: mp 116–118 °C; UV (MeOH): λ_{max} 207 nm (ε 20 584 $cm^{-1}M^{-1}$), 233 (33 683), 266 (14 783), 333 (7547); IR (KBr): ν_{max} 3284, 3068, 2915, 2848, 1696, 1651, 1604, 1581, 1522, 1467, 1449, 1371, 1324, 1295, 1247, 1219, 1232, 1164, 1129, 1040, 1006, 892, 854, 813, 769, 721, 690, 628, 599, 552, 512 cm^{-1}; ^1H NMR (300 MHz, $CDCl_3$): δ 0.87 (t, J = 6.65 Hz, 3H, $CH_2CH_2(CH_2)_9CH_3$), 1.25–1.39 (m, 18H, $CH_2CH_2(CH_2)_9CH_3$), 1.56–1.66 (m, 2H, $NHCH_2CH_2(CH_2)_9CH_3$), 2.21 (s, 3H, $COCH_3$), 3.36–3.43 (m, 2H, $NHCH_2(CH_2)_{10}CH_3$), 6.87 (s, 1H, CONH), 7.14–7.09 (m, 1H, H4), 7.61–7.56 (m, 1H, H5), 8.35 (d, J = 7.84 Hz, 1H, H3), 8.64 (d, J = 8.39 Hz, 1H, H6), 10.96 (s, 1H, NHCO); ^{13}C NMR (75.6 MHz, $CDCl_3$): δ 192.14, 169.16, 162.77 (3 × C=O), 141.95 (ArC), 136.40 (ArCH), 134.32 (ArCH), 122.46 (ArCH), 120.59 (ArCH), 118.66 (ArC), 39.57 ($NHCH_2$), 31.81, 29.54, 29.52, 29.47, 29.42, 29.24, 29.18, 29.13, 26.78, 22.59 ($CH_2(CH_2)_{10}CH_3$), 25.35 ($COCH_3$), 14.02 ($CH_2(CH_2)_{10}CH_3$); HRMS (ESI) *m/z* calculated for $C_{22}H_{34}N_2O_3$ $(M + 1)^+$ 375.5170. Found 375.2622; Anal. Calcd. for $C_{22}H_{34}N_2O_3$: C, 70.55; H, 9.15; N, 7.48. Found: C, 70.84; H, 9.21; N, 7.53%

Hexyl 2-(2-(2-acetamidophenyl)-2-oxoacetamido)acetate, 6b. *N*-Acetyl glyoxylamide peptide mimic **6b** was prepared from 1-acetylindoline-2,3-dione (0.37 g, 2 mmol) and glycine hexyl ester hydrochloride (1 g, 5 mmol) according to GP 2. Purification by gravity column chromatography over silica with CH_2Cl_2 gave the title compound **6b** as off-white flakes (0.31 g, 45%). The solid, recrystallized from hexane *via* slow evaporation of the solvent at room temperature, yielded crystals suitable for X-ray crystal structure determination. **6b**: mp 56–58 °C; UV (MeOH): λ_{max} 191 nm (ε 30 116 $cm^{-1}M^{-1}$), 233 (29 362), 273 (12 824), 341 (6847); IR (KBr): ν_{max} 3319, 2959, 2929, 2856, 1754, 1701, 1644,

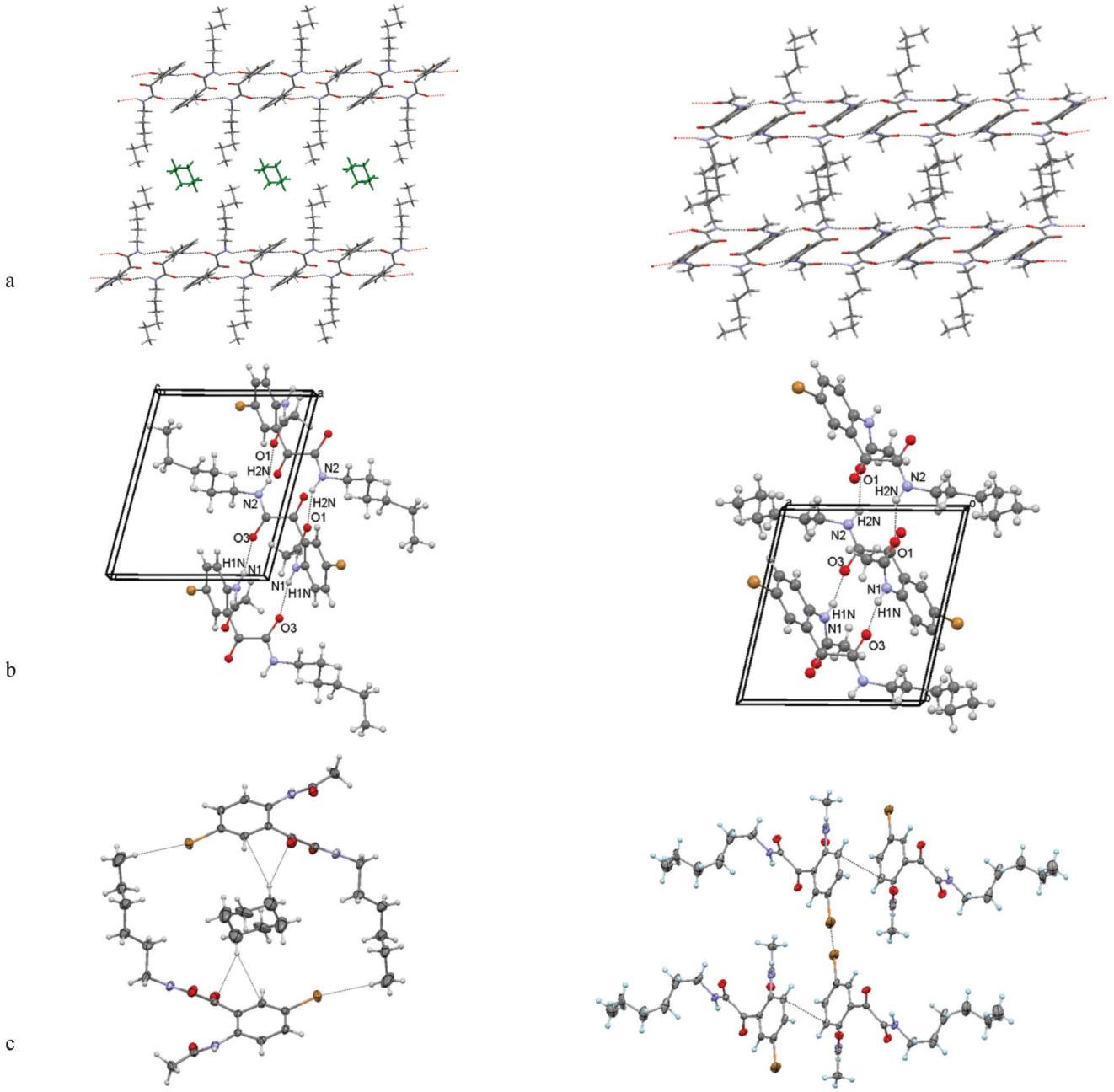

Fig. 6 Crystal packing (a), intermolecular interactions (b) and Br interactions (c) present in **5b-1** (left) and **5b-2** (right).

Table 12 Numerical details of the intermolecular interactions present in **5b-1**

Donor (D)–H···Acceptor (A)	D–H (Å)	H···A (Å)	D···A (Å)	Angle (°)
N1–H···O3[a]=[C10]	0.88	1.94	2.805(6)	169
N2–H···O1[b]=[C7]	0.88	2.06	2.814 (6)	143
C13A–H···O2[c]=[C9]	0.99	2.48	3.169(12)	126
C14A–H···O2[c]=[C9]	0.99	2.59	3.280(14)	127

Equivalent position indicators:[a] 1 − *x* , 1 − *y*, −*z*. [b] 1 − *x*, 2 − *y*, −*z*. [c] −1 + *x*, *y*, *z*.

Table 13 Numerical details of the intermolecular interactions present in **5b-2**

Donor (D)–H···Acceptor (A)	D–H (Å)	H···A (Å)	D···A (Å)	Angle (°)
N1–H···O3[a]=[C10]	0.88	1.94	2.799(4)	166
N2–H···O1[b]=[C7]	0.88	2.05	2.802(4)	142
C11–H11B···O1[b]=[C7]	0.99	2.68	3.224(5)	115

Equivalent position indicators:[a] 2 − *x*, 2 − *y*, 1 − *z*. [b] 2 − *x*, 1 − *y*, 1 − *z*.

1605, 1586, 1533, 1451, 1360, 1322, 1297, 1196, 1096, 1035, 961, 940, 816, 767, 754, 685, 661, 630, 522 cm^{-1}; ^1H NMR (300 MHz, $CDCl_3$): δ 0.88 (t, J = 6.75 Hz, 3H, $CH_2(CH_2)_4CH_3$), 1.26–1.39 (m, 6H, $CH_2CH_2(CH_2)_3CH_3$), 1.63–1.71 (m, 2H, $CH_2CH_2(CH_2)_3CH_3$), 2.22 (s, 3H, $COCH_3$), 4.16 (d, J = 5.48 Hz, 2H, $NHCH_2COO$), 4.19 (t, J = 6.75 Hz, 2H, $COOCH_2(CH_2)_4CH_3$), 7.09–7.14 (m, 1H, Ar-H4), 7.30 (s, 1H, $NHCH_2COO$), 7.57–7.63 (m, 1H, Ar-H5), 8.35 (dd, J = 1.62, 8.10 Hz, 1H, Ar-H3), 8.66

(dd, J = 0.94, 8.55 Hz, 1H, Ar-H6), 10.93 (s, 1H, NHCO); ^{13}C NMR (75.6 MHz, $CDCl_3$): δ 191.02, 169.31, 168.97, 162.84 (4 x C=O), 142.29 (ArC), 136.79 (ArCH), 134.45 (ArCH), 122.57 (ArCH), 120.71 (ArCH), 118.42 (ArC), 66.12 ($COOCH_2(CH_2)_4CH_3$), 41.33 ($NHCH_2COO$), 31.36, 28.47, 25.50, 22.51 ($CH_2(CH_2)_4CH_3$), 25.47 ($COCH_3$), 13.97 ($CH_2(CH_2)_4CH_3$); HRMS (ESI) m/z calculated for $C_{18}H_{24}N_2O_5$ $(M + 1)^+$ 349.1685. Found 349.1180; Anal. Calcd. for $C_{18}H_{24}N_2O_5$: C, 62.05; H, 6.94; N, 8.04. Found: C, 62.05; H, 7.16; N, 8.03%.

Acknowledgements

We thank the Directorate General of Higher Education, Ministry of National Education, Indonesia through the University of Sebelas Maret, Indonesia for a PhD scholarship to Venty Suryanti. We also thank Dr Tom Caradoc-Davies, a Principal Scientist (Australian Synchrotron), for his help in data acquisition.

References

1 J. W. Steed and J. L. Atwood, *Supramolecular Chemistry*, John Wiley & Sons, Ltd., UK, 2nd edn, 2009.
2 C. Janiak, *J. Chem. Soc., Dalton Trans.*, 2000, 3885–3896.
3 C. Janiak and T.G. Scharmann, *Polyhedron*, 2003, **22**, 1123–1133.
4 C. M. Reddy, M.T. Kirchner, R. C. Gundakaram, K. A. Padmanabhan and G. R. Desiraju, *Chem.–Eur. J.*, 2006, **12**, 2222–2234.
5 R. E. Melendez, A. D. Hamilton, *Design of Organic Solids: Hydrogen-Bonded Ribbons, Tapes and Sheets as Motifs*, Springer-Verlag, Berlin, 1998.
6 G. R. Desiraju, *Angew. Chem., Int. Ed. Engl.*, 1995, **34**, 2311–2327.
7 G. R. Desiraju and T. Steiner, *The Weak Hydrogen Bond in Structural Chemistry and Biology*, Oxford Science Publication, Oxford, 1999.
8 S. S. Kuduva, D. Blaser, R. Boese and G. R. Desiraju, *J. Org. Chem.*, 2001, **66**, 1621–1626.
9 C. Greenberg, M. Breneman and J. F. Liebman, *The Amide Linkage: Structural Significance in Chemistry, Biochemistry and Materials Science*, Wiley-IEEE, 2002.
10 D. StC. Black, D. C. Craig and D. B. McConnell, *J. Am. Chem. Soc.*, 1996, **118**, 8148–8149.
11 D. StC. Black, D. C. Craig and D. B. McConnell, *Tetrahedron Lett.*, 1997, **38**, 4287–4290.
12 D. StC. Black, G. C. Condie, D. C. Craig and D. B. McConnell, *Mol. Cryst. Liq. Cryst.*, 2005, **440**, 141–146.
13 W. C. Cheah, D. S. Black, W.K. Goh and N. Kumar, *Tetrahedron Lett.*, 2008, **49**, 2965–2968.
14 W. C. Cheah, K. Wood, D. S. Black and N. Kumar, *Tetrahedron*, 2011, **67**, 7603–7610.
15 T. Le, W. C. Cheah, K. Wood, D. S. Black, M. D. Willcox and N. Kumar, *Tetrahedron Lett.*, 2011, **52**, 3645–3647.
16 L. A. Estroff and A. D. Hamilton, *Chem. Rev.*, 2004, **104**, 1201–1217.
17 J. H. Jung, G. John, M. Masuda, K. Yoshida, S. Shinkai and T. Shimizu, *Langmuir*, 2001, **17**, 7229–7232.
18 F. H. Allen, C. A. Baalham, J. P. M. Lommerse and P. R. Raithby, *Acta Crystallogr., Sect. B*, 1998, **54**, 320–329.
19 R. Paulini, K. Müller and F. Diederich, *Angew. Chem., Int. Ed.*, 2005, **44**, 1788–1805.
20 F. R. Fischer, P. A. Wood, F. H. Allen and F. Diederich, *Proc. Natl. Acad. Sci. U. S. A.*, 2008, **105**, 17290–17294.
21 C. Fäh, L. A. Hardegger, M.-O. Ebert, W. B. Schweizer and F. Diederich, *Chem. Commun.*, 2010, **46**, 67–69.
22 R. Bishop and N. K. Hamer, *J. Chem. Soc. C*, 1970, 1197–1202.
23 L. Fábián, A. Argay, A. Kálmán and M. Báthori, *Acta Crystallogr., Sect. B*, 2002, **58**, 710–720.
24 L. Fábián and A. Kálmán, *Acta Crystallogr., Sect. B*, 2004, **60**, 547–558.
25 G. V. Bhosekar, C. Murali, R. G. Gonnade, M. S. Shashidar and M. M. Bhadbhade, *Cryst. Growth Des.*, 2005, **5**, 1977–1982.
26 A. Anthony, A. Nangia, G. R. Desiraju and M. Jaskólski, *Chem. Commun.*, 1998, 2537–2538.
27 G. R. Desiraju, *Angew. Chem., Int. Ed. Engl.*, 1995, **34**, 2311–2327.
28 G. R. Desiraju and R. Parthasarathy, *J. Am. Chem. Soc.*, 1989, **111**, 8725–8726.
29 T. Sakurai, M. Sundaralingam and G. A. Jeffrey, *Acta Crystallogr.*, 1963, **16**, 354–363.
30 N. Ramasubbu, R. Parthasarathy and P. Murray-Rust, *J. Am. Chem. Soc.*, 1986, **108**, 4308–4314.
31 Bruker, *SADABS*, Bruker AXS Inc., Madison, Wisconsin, USA, 2001.
32 Bruker, *APEX2 and SAINT*, Bruker AXS Inc., Madison, Wisconsin, USA, 2001.
33 G. M. Sheldrick, *Acta Cryst.*, 2008, **A64**, 112–122.
34 C. F. Macrae, I. J. Bruno, J. A. Chisholm, P. R. Edgington, P. McCabe, E. Pidcock, L. Rodriguez-Monge, R. Taylor, J. van de Streek and P. A. Wood, Mercury CSD 2.0 - new features for the visualization, investigation of crystal structures, *J. Appl. Crystallogr.*, 2008, **41**, 466–470.
35 W. Kabschi, *J. Appl. Crystallogr.*, 1993, **26**, 795–800.

